

ASPECT RATIO EFFECTS ON FLOW PAST A BED-MOUNTED EMERGENT CYLINDER

Abhinav Thakurta

Department of Mechanical, Automotive and
Materials Engineering
University of Windsor
401 Sunset Ave,
Windsor, ON, N9B 3P4 Canada
thakurta@uwindsor.ca

John Agyapong Boamah

Department of Mechanical, Automotive and
Materials Engineering
University of Windsor
401 Sunset Ave,
Windsor, ON, N9B 3P4 Canada
boamahj@uwindsor.ca

Vesselina Roussinova

Department of Mechanical, Automotive and
Materials Engineering
University of Windsor
401 Sunset Ave,
Windsor, ON, N9B 3P4 Canada
vtr@uwindsor.ca

Ram Balachandar

Department of Civil and Environmental Engineering
University of Windsor
401 Sunset Ave,
Windsor, ON, N9B 3P4 Canada
rambala@uwindsor.ca

ABSTRACT

This study investigates the impact of aspect ratio (AR) on the wake generated by flow past a bed-mounted emergent cylinder in an open channel. Here, aspect ratio is defined as the ratio of flow depth (H) to cylinder diameter (d). Detailed velocity measurements were conducted using a planar particle image velocimetry (PIV) system to examine the turbulent wake structures for aspect ratios ranging from 1.7 to 6.7. The research aims to explore turbulent structures in the near wake region and assesses the impact of cylinder AR for Reynolds number (Re_d) exceeding 900, where Re_d is based on cylinder diameter and approach flow bulk velocity (U_m). The study builds upon prior investigation carried out by Heidari et al. (2017) on a bed-mounted slender cylinder with AR = 11. The results indicate distinct flow features attributed to different aspect ratios, with reduced energy contribution observed in the near-bed plane despite continued vortex shedding, as revealed by a Proper Orthogonal Decomposition (POD) analysis.

INTRODUCTION

The fluid dynamics around wall-mounted emergent cylinders is crucial due to its wide range of engineering and environmental flow applications including bridge pier design, flow past vegetation in rivers, coastal structures, and pin fins in heat transfer processes. In this study, the near wake of an emergent wall-mounted cylinder in a shallow flow is considered. A flow is referred to as shallow when the horizontal length scale is significantly larger than the vertical scale or the depth of the flow (Jirka et al., 2004; Balachandar et al., 2000). It is well recognized that the shallow wake of a wall-mounted cylinder is very different from the wake of an infinitely long circular cylinder. The shallow near-wake characteristics have been found to exhibit intricate wake characteristics. Chen and Jirka (1995) investigated the case where the cylindrical bluff body diameter, was greater than the water depth ($d/H > 1$) and classified the shallow near-wake structures into three categories: von Kármán vortex street with an oscillating vortex shedding mechanism, an unsteady wake bubble with growing instabilities downstream and a steady wake bubble followed by turbulent wake with no growing instabilities. Ingram and Chu (1987) observed that bed friction effects become important in shallow wakes, and they defined a stability parameter $S = C_f d/H$, where C_f is the skin friction coefficient. The stability parameter, S is a relative

measure of the competing effects between the bed friction and the transverse shear in the shallow wake. Their research demonstrated dissimilarities of the wake compared to the bluff body wake in deep flow, specifically for bluff bodies with small aspect ratios ($AR = H/d < 0.6$). Due to the presence of the bed, flow past an emergent bed-mounted cylinder is characterized by additional flow structures such as the base vortices and upwash flow.

Akilli and Rockwell (2002) investigated the near wake of a small aspect ratio ($AR < 2$) emergent cylinder at $Re_d = 10^4$. It was observed that the concentration of vorticity and Reynolds stress distributions occur in a narrow region close to the bed but become broader as the free surface is approached. Kirkil and Constantinescu (2012) examined the dynamics of vortical structures behind a circular cylinder ($AR = 1.12$) mounted on a smooth bed in an open channel flow using large eddy simulation (LES). Their findings revealed that some parts of the horseshoe vortex legs were directed towards the axis of symmetry at approximately $1.7d$ behind the cylinder, near the bed, and maintained their coherence further downstream. Rao et al. (2004) visually examined the wake structure behind cylinders with large aspect ratios ($AR = 7.0 - 11.7$). Their study demonstrated that the structures in the junction flow, particularly the horseshoe vortex (HV), influence the dynamics of the shear layer and von Kármán vortices throughout the depth of the flow. Heidari et al. (2017) investigated the complex wake generated by an emergent cylinder with a large aspect ratio ($AR = 11$) in a shallow open channel flow at two different flow Reynolds numbers. They observed the presence of significant vertical velocity and turbulence intensities near the bed in the vertical midplane.

The previous investigations on emergent bed-mounted cylinder encompass studies, with either a large or small aspect ratios. A comprehensive analysis is needed to understand the impact of the intermediate aspect ratio on the wake dynamics of circular wall-mounted cylinders piercing the free surface. The constrained flow depth effectively eliminates the flow structures that are formed at the free end of the cylinder, thereby altering the wake, and eliminating the downward flow behind the cylinder. The separated shear layers on the sides of the cylinder extend to the free surface, and the LES study of Kawamura et al. (2002) observed an insignificant effect on the near wake flow for small Froude numbers ($Fr < 0.5$). In the present study, we alter

the diameter of the cylinder to achieve three different aspect ratios, while ensuring that the submergence ratio δ/H remains close to one. The objective of this study is to gain further understanding of the effects of aspect ratio on wake flow and coherent structures for an emergent cylinder with $Fr = 0.3$. The present experimental work builds upon the findings of Heidari et al. (2017), who conducted separate experiments on cylinder with $AR = 11$.

EXPERIMENT SETUP

Particle image velocimetry (PIV) experiments were conducted in a recirculating water flume at the University of Windsor. The flume has a rectangular cross-section with 16 m length, 1.2 m width, and 0.8 m height. An acrylic transparent smooth plate, 1.5 m long and spanning the width of the flume is positioned parallel to the flume bed. The smooth plate was located 8 m from the entrance of the channel and the cylinder was mounted 0.7 m from the beginning of the plate. Three cylinders with diameters $d = 0.0127$ m, 0.026 m and 0.050 m at constant flow depth $H = 0.085$ m are used at emergent conditions. The schematic of the experimental setup is shown in Figure 1.

The PIV system was used to obtain detailed velocity measurements in the near wake region for each AR in the vertical centre plane ($x - y$) and three horizontal planes ($x - z$) as shown in Figure 1. The PIV system included dual pulse Nd:YAG laser (Litron Nano) with a wavelength of 532 nm and 135 mJ/pulse energy. Cylindrical lenses with focal lengths of 15 mm and 25 mm were attached to the laser, creating a laser sheet with an approximate thickness of 1 mm. PIV images from two PowerViewPlus 8 MP CCD cameras with a resolution 3312 pixels \times 2488 pixels were acquired simultaneously to capture the extended streamwise vertical/horizontal FOVs behind the cylinder. The cameras were equipped with Nikon AF NIKKOR 50 mm lenses. The cameras operated in dual capture mode and were synchronized with a laser pulse repetition frequency of 2.42 Hz for vertical central plane and 3.36 Hz for all horizontal planes. The field-of-view of each camera was set to $1.7H \times 1H$ in the x - and y - directions with a small overlap of $\sim 0.01m$. The flow was seeded with 10 μ m spherical silver-coated hollow glass spheres with an 1100 kg/m³ density. A total of 2000 image pairs were captured in each plane for all ARs.

PIV images were processed using open-source MATLAB PIVlab software (Thielicke et al., 2014). Initial background subtraction was followed by the contrast-limited adaptive histogram equalization (CLAHE) technique. The image processing occurred initially, using an interrogation window of 64×64 pixels following by a smaller 32×32 pixels interrogation area, with a spatial overlap of 50% in each direction. The final process yielded an interrogation area of 16×16 pixels. The final FOVs behind the cylinder was 145 mm \times 88 mm with the resulting vector spacing of 0.75 mm in each direction.

Table 1 summarizes details for the flow parameters for all experiments. The incoming turbulent boundary layer thickness

(δ), friction velocity (u_τ), and bulk velocity (U_m) are determined from a separate PIV measurement in the absence of the cylinder. The bulk velocity for all AR cases is 0.29 m/s. The turbulence intensity of the flow in the absence of the cylinder was 1.8%. The blockage ratios (BR) are also included in Table 1, which are small and not expected to influence the results.

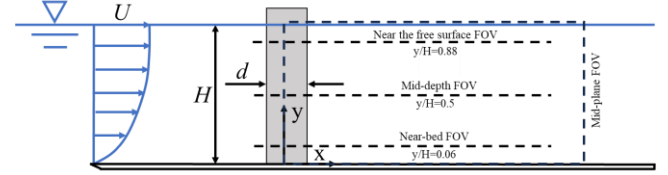


Figure 1. Schematic of the experimental set-up including PIV vertical midplane (at $z/d = 0$) and the three horizontal planes at $y/H = 0.06, 0.5$ and 0.88 .

RESULTS AND DISCUSSION

The results are divided into two sections: (i) an overview of the mean wake flow features is presented using the time-averaged flow to describe the effect of the AR in vertical and horizontal planes; and (ii) the discussion of the low-order representations of the wake dynamics using the proper orthogonal decomposition (POD) for the near-bed horizontal plane is analysed.

Wake analysis in vertical plane.

Figure 2a shows the contours of the streamwise mean velocity, normalized by bulk velocity (U_m), in the central vertical plane ($z/d = 0$) downstream of the cylinders for aspect ratios of 1.7 (AR1), 3.3 (AR2) and 6.7 (AR3). The U/U_m velocity contours are superimposed with the averaged streamtraces to illustrate the flow pattern. The presence of the cylinders causes perturbations in the flow, which are observed throughout the water depth. The velocity fields indicate that the wake of the piercing cylinder can be divided into two zones, regardless of the aspect ratio. The first zone starts immediately behind the cylinder and includes both reverse flow and the recirculation region. Analysis of the streamtraces reveals different flow topologies with significant vertical motion in the wake of all cylinders. However, the effect of free surface confinement and the flow blockage area of the emergent cylinders causes the flow to move towards the cylinder in the vertical midplane.

The flow undergoes a counterclockwise recirculation near the cylinder wall and the bed, as seen in both AR1 and AR2 cases. However, in the case of $AR3 = 6.7$, a weak clockwise recirculation is observed, as depicted in Figure 2.

Table 1 Incoming flow parameters

Case	d (mm)	H (mm)	U_m (m/s)	AR	Re_d	Re_H	BR (%)	δ (mm)	U_τ (m/s)	δ/H
AR1	50.00	85.00	0.29	1.7	14500	24700	4.5	76	0.0152	0.89
AR2	25.50	85.00	0.29	3.3	7400	24700	2.3	76	0.0152	0.89
AR3	12.70	85.00	0.29	6.7	3700	24700	1.2	76	0.0152	0.89

In Figure 2a, the wake behind the cylinders with AR1 and AR2 is longer and occupies the entire flow depth in the vertical central plane. In contrast, a shorter wake is formed behind the cylinder with AR3. The streamtraces for AR3 do not show a well-defined recirculation region, as the flow in the wake overcomes the disturbance caused by the slender cylinder. The second zone mainly comprises a mean flow with $U/U_m > 0$. It is observed that the location of the source of the vertical motion along the x/d direction varies with the aspect ratio. For AR1, it begins at $x/d = 2.5$, for AR2, the location shifts towards $x/d = 2$ and for the case of AR3, the location further shifts to $x/d = 1$. It is evident from Figure 2a that the reverse flow region exhibited by the blue contour decreases with an increase in the aspect ratio. The aspect ratio exerts a significant influence on the reverse-flow region behind the wall-mounted cylinders. For instance, the maximum backflow velocity in this study decreased from $-0.42U_m$ to $-0.08U_m$ as the aspect ratio increases from AR1 to AR3. In the case of cylinders with low AR, an area of recirculation is observed near the bed and close to the cylinder. Akilli and Rockwell (2002) observed a similar flow topology reminiscent of the spanwise-oriented vortex. The strength and vertical position of the recirculation area depends on the aspect ratio. For the case of AR1, the centre of the recirculation region is positioned at $x/d = 0.86$ and $y/H = 0.34$. However, for an aspect ratio AR2, the centre of the recirculation area moves closer to the cylinder and near the bed at $x/d = 0.8$ and $y/H = 0.19$. For the aspect ratio AR3, the centre of recirculation rises to $x/d = 1.28$ and $y/H = 0.85$. The presence of reverse flow near the free surface is evident when the aspect ratio is low, but this

diminishes as the aspect ratio increases. These observations further emphasize the changes in the flow pattern in the near wake caused by varying aspect ratios.

The aspect ratio also influences the wake length in the vertical plane as the shear layers separating from the sides of the cylinder attach at a shorter distance in cylinders with a high aspect ratio than in cylinders with a low aspect ratio. The solid red line depicts the boundary of the recirculation wake region at $U/U_m = 0$ for different aspect ratios.

Figure 2b presents the contours of the vertical mean velocity (V/U_m) in the near-wake region, in the central vertical plane ($z/d = 0$), downstream of the cylinder. The region with $V/U_m < 0$ can be seen behind the cylinder, as illustrated by the contours. For aspect ratios AR1 and AR2, flow in the downward direction is observed at $0.5 < x/d < 0.9$, however, this downward flow diminishes for aspect ratios AR3. This downward flow is due to the recirculation as discussed earlier and diminishes with increase in the aspect ratio. Additionally, as we move along the streamwise direction, a significant upward flow is observed in all cases. This upward flow can be attributed to the influence of vortex structures that form at the base of the cylinder. These base vortices are associated with the upward-directed flow or upwash flow that occurs behind the cylinder. This upwash flow induces a significant vertical motion, as can be seen in Figure 2b (Heidari et al. 2017; Sumner et al. 2004; Wang et al. 2009). Near the wall, increase in aspect ratio results in the increase of the upwash flow that suggests an increase in the base vortices (Okamoto 1992).

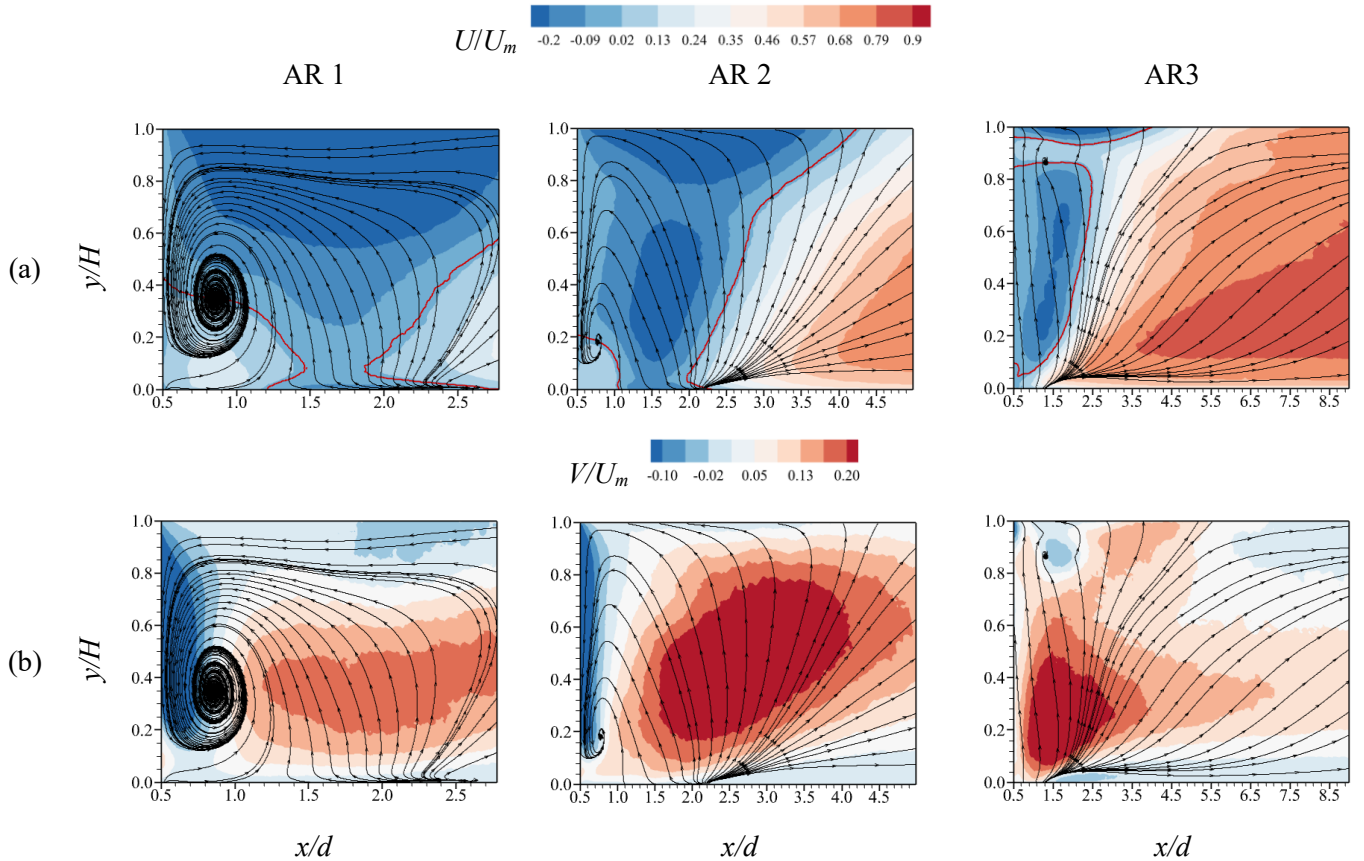


Figure 2. Contours of (a) the streamwise velocity (U/U_m) and (b) the vertical velocity (V/U_m). The streamtraces and the red solid line represents the boundary of recirculation region at $U/U_m = 0$ are superimposed.

The contours show that an increase in the aspect ratio induces a noticeable increase in the vertical component of the flow velocity. Moreover, the region where the vertical component of the flow velocity is high ($V/U_m \geq 0.20$) is not present in the case of AR1, but it can be observed in higher aspect ratios. Specifically, in the case of AR2, the high vertical velocity region starts at $x/d = 1.5$ and extends till $x/d = 4$. Furthermore, for higher aspect ratios such as AR3, the high vertical velocity region shifts towards the cylinder, beginning at $x/d = 0.9$ and 0.7 respectively. As the aspect ratio increases, the wake behind the cylinder decreases, resulting in a shrinking of the region with high-velocity contour along the streamwise direction.

Wake analysis in the horizontal planes

Figure 3 illustrates the streamwise mean velocity contours in the near bed ($y/H = 0.06$) and mid-depth ($y/H = 0.50$) planes for the three ARs. The streamtraces are superimposed on the mean velocity contours to highlight the wake flow topology. A symmetric wake pattern is observed in all cases with a recirculation region on either side of the symmetry plane. The streamtraces depict the recirculation behind the cylinder which is influenced by the aspect ratio. The red line ($U/U_m = 0$) denotes the reverse flow region behind the cylinder. This region varies across the planes for different aspect ratio indicating a significant influence of the bed and the bluff body on the wake characteristics. In the near the bed plane, the revers flow region is detached from the back of the cylinder for AR1 and AR2 coinciding with the region of $U/U_m < 0$ as seen in Figure 2a.

In the mid-depth plane ($y/H = 0.5$), the length of the recirculation zone behind the cylinder is observed to reduce with an increase in the aspect ratio. In the case of AR1, the length of

the recirculation region along the plane of symmetry is equal to $3d$ while for AR2, it is $2.6d$ and $2d$ for AR3. This can be attributed to the fact that the flow travels larger distance in the case of AR1 for the reattachment behind the cylinder as compared to AR2 and AR3. This results in a long recirculation length in the case of AR1. However, due to the cylinder's slenderness for AR3, the wake closes at $x/d \approx 2.2$, resulting in having the shortest recirculation region among the three AR cases. In the near-bed plane, the bed friction effect is dominant, resulting in a shorter wake region for all cases. In all three cases, the flow tends to move inward to form the recirculation region. Similar conclusion can be drawn from the mid-depth plane for the wake behind the cylinder which is strongly influenced by the aspect ratio.

Proper Orthogonal Decomposition (POD)

Proper Orthogonal Decomposition (POD) was applied to the PIV fluctuating velocity fields in the near-bed ($x - z$) plane to study the onset of the vortex-shedding phenomenon under the competing effect of bed friction. The POD was computed using the snapshot method (Sirovich, 1987) and offers a qualitative insight into the dominant flow features associated with each mode and their variations. Furthermore, the low-order modes contain most of the total turbulent kinetic energy (TKE), and they are associated with energetic large-scale structures, while the high-order modes are associated with small-scale structures. In this study, the discussion focuses on the first two most energetic POD modes for the three aspect ratios.

Figure 4 illustrates the distribution of the percentage of TKE contribution by the first two POD modes across different aspect ratios. The results show that AR strongly influences the relative energy content of the first two modes in the near bed plane.

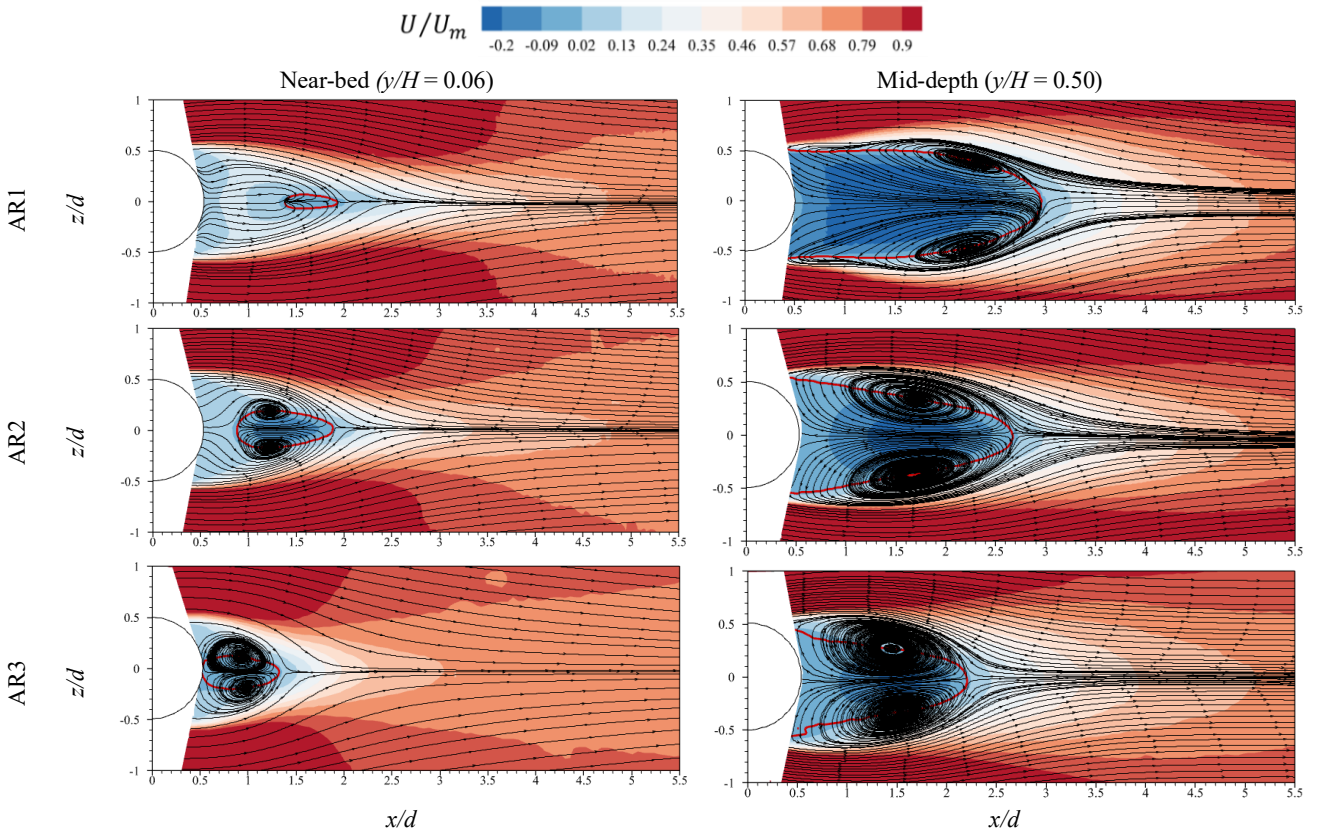


Figure 3. Contours of the streamwise mean velocity (U/U_m) superimposed by the streamtraces. The red solid contour line represents the boundary of recirculation region at $U/U_m = 0$ for different aspect ratios.

The highest energy is recorded for the first mode, gradually decreasing for the second mode. In addition, AR1 exhibits the highest cumulative energy of 15.5% for the first two POD modes, while AR2 and AR3 exhibit 13.5% and 7.3%, respectively. The drop in cumulative energy from AR2 to AR3 is 6%, which is three times the drop observed from AR1 to AR2. This observation aligns with the mean streamwise velocity in the near-bed plane, where the shear layers interact closer to the cylinder in AR3. Near the bed, the contribution of the large-scale structures generated by a slender bluff body is less compared to the lower AR cases. Consequently, maintaining identical approach flow conditions for all ARs, an increase in the aspect ratio leads to a reduction in cumulative energy.

Figure 5 shows the spatial distributions of the normalized streamwise eigenfunction, $\phi_U/\phi_{U_{max}}$ of POD modes 1 and 2 for all AR cases. The contours for the two POD modes exhibit anti-symmetric spatial distributions for all AR cases. Previous studies which have examined the TKE distribution of the 2D circular cylinder have found that the first two POD modes make up a majority of the total TKE contribution (Van Oudheusden et al. 2005) and have been associated with vortex shedding. The present POD modes confirm the presence of the vortex shedding in the near bed plane. The repeating pattern associated with these vortices (Mode 1) is initiated at different streamwise locations for different aspect ratios. In the case of AR1, the concentrated energy region for mode 1 is observed approximately at $x/d \approx 3$, while for AR2 and AR3 it is shifted closer to the cylinder at $x/d \approx 2$ and $x/d \approx 1$, respectively. These streamwise locations coincide with the end of the wake recirculation bubble as shown

in Figure 3. The lower aspect ratio results in the shear layers interacting at a farther distance, which decreases with an increase in aspect ratio. It appears that the similar discussion applies to mode 2, where the spatial concentration of energetic modes is farthest for AR1 and closest for AR3.

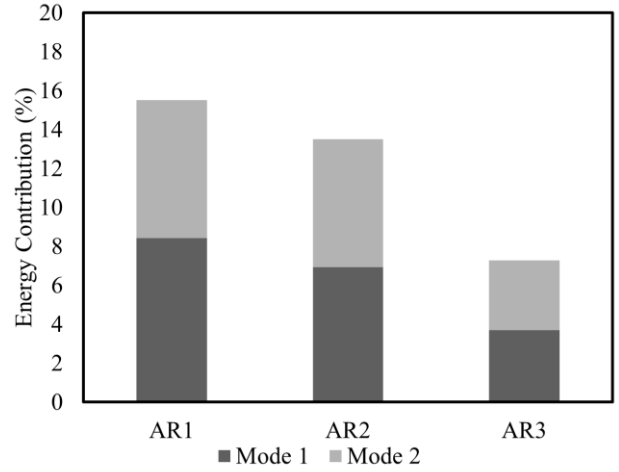


Figure 4. Energy per modes for different aspect ratios for the horizontal near-bed plane.

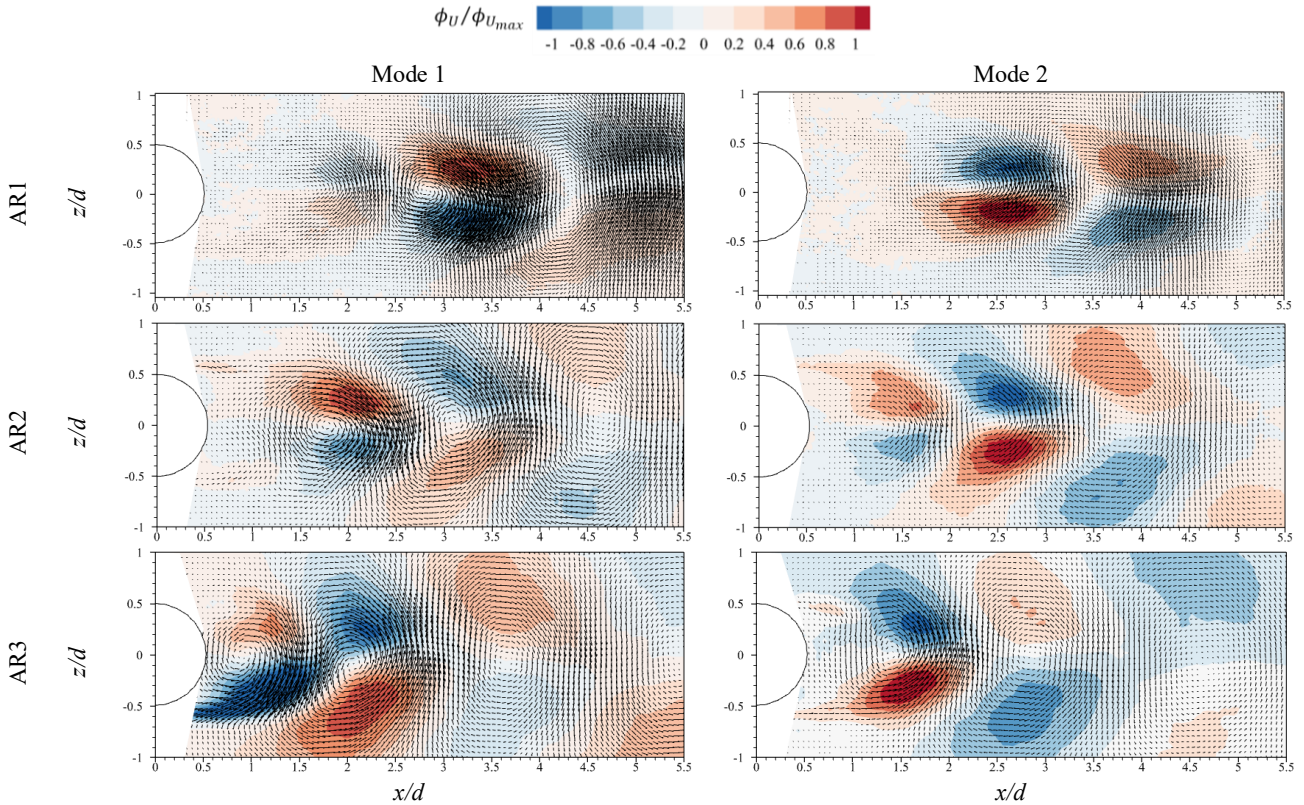


Figure 5. Contours of the streamwise mean velocity (U/U_m) superimposed by the streamtraces. The red solid contour line represents the boundary of recirculation region at $U/U_m = 0$ for different aspect ratios.

Near the wall, the spatial wavelength (λ) of the anti-symmetric vortex shedding is examined by measuring the distance between the peaks of alternating (positive and negative) regions of the spanwise component of the POD modes, ϕ_w (not shown here due to page limit). The distance between two successive peaks corresponds to half the local wavelength ($\lambda/2$). It was found that the spatial wavelength of the vortices for AR1 is $\lambda = 3.2d$ (Mode 1) and reduces to $2.6d$ (Mode 1) for AR2 and AR3. Essel et al. (2021) reported a value of the Strouhal number, $St_H \approx 0.2$ for a submerged cylinder of AR = 7 in the near bed plane. Since their cylinder AR is close to the case presented here, we use similar $St_H = 0.2$ to compute the convective velocity of the vortices in the wake. Near the wall, the convective velocity of the vortices for AR1 is $0.46U_m$ and reduces to $0.38U_m$ for AR2 and AR3. An increase in the convective velocity of the vortices shed behind the cylinder at AR1 is obtained in the near-bed plane.

CONCLUSION

Planar PIV measurements were utilized to analyze velocity fields across three aspect ratios (AR1 = 1.7, AR2 = 3.3 and AR3 = 6.7) in the current study. Investigation of the velocity field behind circular cylinders with differing aspect ratios provided insights into wake characteristics under shallow flow conditions for emergent cylinders piercing the free surface. The experiments are carried out for three different cylinder diameters at fixed approach flow $Re_H = 24700$. The PIV measurements were conducted in the wall-normal (x - y) plane at the symmetry ($z/d = 0$) and in the three horizontal (x - z) planes of each cylinder to capture the structures in the near wake region. The time averaged velocity fields demonstrate that both the bed and the bluff-body induce three-dimensional effects into the flow field behind the cylinder, a phenomenon significantly influenced by the aspect ratio. Notably, an increase in the aspect ratio leads to a reduction in downward vertical velocity behind the cylinder, bringing the recirculation bubble closer to the cylinder. Proper orthogonal decomposition was employed to extract the highest energy modes, revealing a decrease in energy contribution with increasing aspect ratio. In the near bed plane, POD analysis showed that the von Karman vortices are present for all ARs. However, vortex shedding is initiated at different streamwise locations for different aspect ratios. These findings emphasize the role of aspect ratio in modifying flow dynamics around the cylinder.

REFERENCES

- Akilli, H. and Rockwell, D. "Vortex formation from a cylinder in shallow water," *Phys. Fluids* 14(9), 2957–2967 (2002).
- Balachandar, R., Ramachandran, S., and Tachie, M.F., "Characteristics of shallow turbulent near wakes at low Reynolds numbers," *J. Fluids Eng.* 122(2), 302–308 (2000).
- Chen, D., and Jirka, G.H., "Experimental study of plane turbulent wakes in a shallow water layer," *Fluid Dyn. Res.* 16(1), 11–41 (1995).
- Essel, E. E., Tachie, M. F., and Balachandar, R. "Time-resolved wake dynamics of finite wall-mounted circular cylinders submerged in a turbulent boundary layer," *Journal of Fluid Mechanics*, 917, A8. (2021)
- Heidari, M., 2016, Wake characteristics of single and tandem emergent cylinders in shallow open channel flow, Ph.D. Thesis, University of Windsor, Windsor, ON.
- Heidari, M. Balachandar, R. Roussinova, V. and Barron R. M., "Characteristics of flow past a slender, emergent cylinder in shallow open channels," *Phys. Fluids* 29(6), 065111 (2017).
- Jirka, G. H., and Uijttewaai, W. S., "Shallow Flows: Research" Presented at the International Symposium on Shallow Flows (Taylor & Francis, Delft, The Netherlands, 2003-2004).
- Kawamura, T., Mayer, S., Garapon, A. and Sorenson, L., "Large Eddy Simulation of a Flow Past a Free Surface Piercing Circular Cylinder," *J. Fluids Eng.* Mar 2002, 124(1): 91-101 (2002).
- Kirkil, G. and Constantinescu, G., "A numerical study of the laminar necklace vortex system and its effect on the wake for a circular cylinder," *Phys. Fluids* 24(7), 073602 (2012).
- Okamoto, T. and Sunabashiri, Y. "Vortex shedding from a circular cylinder of finite length placed on a ground plane," *J. Fluids Eng* 114, 512–521 (1992).
- Rao, S. K., Sumner, D. and Balachandar, R., "A visualization study of fluid structure interaction between a circular cylinder and a channel bed," *J. Visualization* 7(3), 187–199 (2004).
- Summer, D., Heseltine, J. L., and Dansereau, O. J. P., "Wake structure of a finite circular cylinder of small aspect ratio," *Exp. Fluids* 37, 720–730 (2004).
- Thielicke, W. and Stamhuis, E., "PIVlab – towards user-friendly, affordable and accurate digital particle image velocimetry in MATLAB", *Journal of Open Research Software*, 2(1), e30 (2014)
- Van Oudheusden, B. W., Scarano, F., Van Hinsberg, N. P., and Watt, D. W., "Phase-resolved characterization of vortex shedding in the near wake of a square-section cylinder at incidence," *Experiments in Fluids*, 39(1), 86–98 (2005)
- Wang, H. F. and Zhou, Y., "The finite-length square cylinder near wake," *Journal of Fluid Mechanics*, 638, 453–490. (2009).